*Bull. Mater. Sci.* (2019) 42:133
https://doi.org/10.1007/s12034-019-1811-7



# Antibacterial, antioxidant properties of *Solanum trilobatum* and sodium hydroxide-mediated magnesium oxide nanoparticles: a green chemistry approach

**S NARENDHRAN*, M MANIKANDAN and P BABY SHAKILA**
Department of Bioscience, Sri Krishna Arts and Science College, Sugunapuram, Kuniamuthur P.O., Coimbatore 641008, India
*Author for correspondence (narendhransumathi@gmail.com)

MS received 18 May 2018; accepted 28 January 2019; published online 25 April 2019

**Abstract.** A comparative study of *Solanum trilobatum*-mediated magnesium oxide (St-MgO) nanoparticles (NPs) and sodium hydroxide-mediated MgO (Che-MgO) NPs are synthesized using magnesium nitrate precursor. The characterization analyses, such as ultraviolet–visible spectroscopy (UV–Vis), Fourier transform infrared spectroscopy (FTIR), X-ray diffraction (XRD), energy-dispersive X-ray diffraction (EDX), scanning electron microscopy (SEM) and particle-size analysis were carried out. To determine the antioxidant activity of MgO NPs by 2,2-diphenyl-1-picrylhydrazyl (DPPH) method and antibacterial activity against *Escherichia coli* (MTCC: 912), *Bacillus subtilis* (MTCC: 121) and *Streptococcus pyogenes* (MTCC: 1925), was performed by the well-diffusion method. The UV–Vis analysis of St-MgO, Che-MgO confirmed the formation of MgO NPs that have a broad absorption peak at 362 and 374 nm, respectively. IR spectrum of synthesized St-MgO and Che-MgO exhibits a high-intensity band at 440 and 460 $cm^{-1}$, respectively. XRD analysis indicates that synthesized St-MgO, Che-MgO were crystal in nature and EDX confirmed the composition of MgO-NPs. SEM analysis revealed that St-MgO and Che-MgO NPs were spherical in shape without aggregation. Particle-size analysis confirmed that the average particle sizes of St-MgO and Che-MgO NPs were 30 and 42 nm, respectively. DPPH assay of St-MgO NPs has higher absorbance value, which indicates the high antioxidant capacity compared with ascorbic acid. St-MgO NPs are effective against bacterial pathogens, such as *E. coli* (16.66 ± 0.66), *B. subtilis* (16.00 ± 0.88) and *S. pyogenes* (13.66 ± 2.08) at 100 mg $ml^{-1}$ concentration when compared with Che-MgO and the control ($P < 0.001$). Thus, the result suggested that safer use of biologically synthesized MgO NPs can act as effective antioxidant and antibacterial agents in the field of biomedicine.

**Keywords.** Antibacterial activity; antioxidant activity; magnesium oxide nanoparticles; *Solanum trilobatum*.

## 1. Introduction

Nowadays, researchers have developed exciting new materials that are nanosized to progress towards unique and tunable properties of the applied materials. An important aspect of nanoscience is related to design experimental methods for the synthesis of nanoparticles (NPs) with different chemical compositions, sizes, shapes and properties. Recently, researchers have tried to find biological methods for the synthesis of NPs that will act as alternatives to chemical or physical methods. Biological methods for the production of NPs are considered safe and environmentally friendly; they are also cost-effective and ensure the complete elimination of toxic chemicals. In addition, the synthesis of NPs using biological means, especially plants, is biocompatible, as they secrete functional biomolecules which actively reduce metal ions.

Magnesium oxide (MgO) NPs are important materials used in catalysts, photonic and electronic devices. MgO particles are inorganic compounds with wide band gaps. It has low heat capacity, high melting point and highly functional. Therefore, it is used for insulation application in various areas [1,2]. MgO NPs act as bactericidal agents because the surface of the particle is synthesized with superoxide anion. Al-Hazmi *et al* [3] recognized that MgO NPs have antibacterial activity due to their size, shape and surface properties. Due to their smaller size, nanomaterials have novel properties, which is different from others [4,5]. Bhatte *et al* [5] demonstrated that the antimicrobial activity of MgO NPs of size from 4 to 10 nm is efficient as bactericidal agents. Doss *et al* [6] explained that particle size < 40 nm has increased antibacterial efficacy.

MgO NPs are synthesized by various methods that include vapour liquid solid, electrochemical process, colloidal micelles, micro oven and ultrasonic. Recently, most researchers follow biological synthesis of NPs rather than physical and chemical methods. They consider that the biological synthesis of NPs are eco-friendly, cost-effective and with low toxicity [7]. In biological synthesis, functional biomolecules of plant metabolism reduce the metal ion [8]. In recent

reports, biological synthesis of MgO NPs from neem, *Clitoria ternatea*, *Parthenium* and *Brassica oleracea* have been carried out successfully [9–11]. Despite the availability of much less information about green route synthesis of MgO NPs, it is still an unknown area and requires further exploration. In the previous investigation, Krishnamoorthy *et al* [11] demonstrated that the green route synthesis of MgO NPs has antibacterial activity against foodborne pathogens.

MgO NPs are safe materials to humans. Inorganic antimicrobial agents (MgO, ZnO, etc.) have a high inhibition rate against various Gram-positive and Gram-negative bacteria, which is a safe and stable material when compared to organic antimicrobial agents. In the medical field, MgO material showed promising application for bone regeneration, sore stomach, relief of heartburn and tumour treatment [12–14]. *Solanum trilobatum* L. belongs to the family Solanaceae. This medicinal plant is used to treat asthma, tuberculosis, respiratory and liver diseases, because it contains a rich amount of nutrients [15]. Phytochemicals like sobatum, solaine, solasodine and glycoalkaloid are the major constituents responsible for antimicrobial and anticancer activities [16]. This plant contains a high percentage of alkaloids and carbohydrates that stimulates a strong immune effect. Due to these overall properties of *S. trilobatum*, it is a good candidate for the synthesis of NPs [17]. In biological synthesis, *S. trilobatum* extract is used to synthesize titanium, silver [18] and palladium NPs [19].

MgO NPs are highly ionic nanoparticulate metal oxides with extremely high surface areas and unusual crystal morphologies. Nanoscale MgO possesses unique optical, electronic, magnetic, thermal, mechanical and chemical properties due to its characteristic structures. MgO is an important functional metal oxide that has been widely used in various fields, such as catalysis, refractory materials, paints and superconductors. Review of literature reveals that there are several methods for the synthesis of nano-sized MgO particles, including the sol–gel method, chemical gas-phase deposition, laser vapourization, hydrothermal synthesis and combustion aerosol synthesis. Biological methods for the synthesis of MgO NPs with the use of plant materials have not been widely exploited.

In this present study, we investigate green route synthesis of MgO NPs using *S. trilobatum* (St-MgO) aqueous extract and chemical synthesis (Che-MgO) of MgO NPs by co-precipitation method. The crystalline and morphology characters of St-MgO and Che-MgO were analysed using ultraviolet–visible spectroscopy (UV–Vis), Fourier transform infrared spectroscopy (FTIR), X-ray diffraction (XRD), energy-dispersive diffraction X-ray (EDX), scanning electron microscopy (SEM) and particle-size analysis. To determine antibacterial activity of green and chemical MgO NPs, the well-diffusion method was performed against test organisms like *Escherichia coli* (MTCC: 912), *Bacillus subtilis* (MTCC: 121) and *Streptococcus pyogenes* (MTCC: 1925).

## 2. Materials

*S. trilobatum* plants were collected from Avarampalayam region, Coimbatore, Tamil Nadu, India. Chemicals used in this experiment were of analytical grade, purchased from Sigma Aldrich. Bacterial pathogens (*E. coli* MTCC 912, *B. subtilis* MTCC 121 and *S. pyogenes* MTCC 1925) were obtained from IMTech, Chandigarh, India. The bacterial pathogens are subcultured and maintained in nutrient agar media for future use.

## 3. Methodology

### 3.1 *Synthesis of St-MgO and Che-MgO*

*S. trilobatum* leaf was washed with distilled water; shade dried for 5 days; powdered using mortar and pestle. A weight of

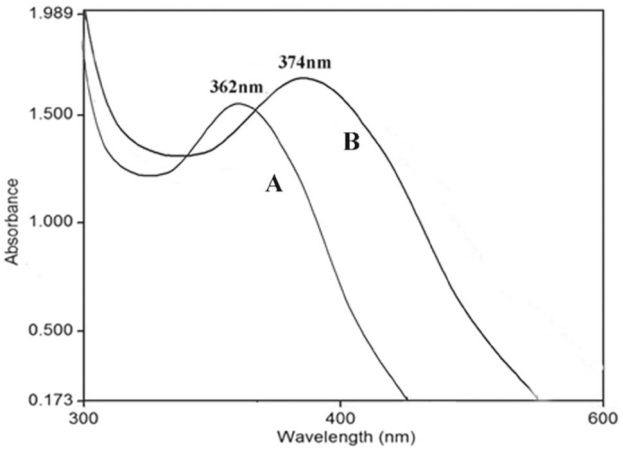


**Figure 1.** UV–Vis analysis of (**A**) *S. trilobatum*-mediated MgO NPs observed at 362 nm and (**B**) magnesium nitrate-mediated MgO NPs observed at 374 nm.

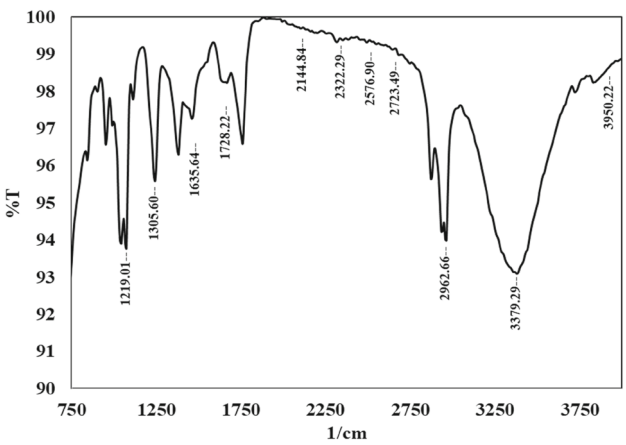


**Figure 2.** FTIR analysis of *S. trilobatum* leaf aqueous extract shows the presence of aliphatic amine, alkanes, unsaturated ester, alkynes, carboxylic acid, amines, alcohol and phenol functional group.

1 g of powdered leaf sample was dissolved in 100 ml of distilled water and heated at 100°C for 5 min. After heating, the sample was filtered with Whatman filter paper and the crude extract was stored for further use. A 50 ml of crude plant extract was added (dropwise) to a beaker, which contained 50 ml magnesium nitrate (0.5 M) solution under magnetic stirring for 4 h until the formation of precipitate settled in the bottom of the conical flask. This precipitate was centrifuged at 5000 rpm for 5 min and the pellets were collected. This precipitate was further purified by washing with Millipore water and ethanol for several times to remove impurities. After the purification step, the precipitate was annealed at 400°C for 8 h and was finely powdered by using mortar and pestle. The final product was stored in a screw-capped bottle for further use.

To synthesize Che-MgO NPs, a 0.5 M magnesium nitrate ($MgNO_3$) and 0.1 M sodium hydroxide (NaOH) were prepared in double-distilled water. A 100 ml of $MgNO_3$ solution was added dropwise to a beaker that contained 100 ml of NaOH solution placed in a magnetic stirrer with high-speed stirring. After 20 min of stirring, the beaker was kept for 2 h undisturbed for the settlement of the precipitate. The precipitated Che-MgO NPs washed with Millipore water was followed by ethanol washing until the removal of impurities and then vacuum dried at 80°C in a hot air oven. Then Che-MgO NPs were transferred to airtight screw-capped bottle for further analysis [9].

### 3.2 *Characterization of St-MgO and Che-MgO*

The optical density and band gap energy were determined by UV–Vis spectroscopy (UV-2450, Shimadzu). The crystalline structure of magnesium NPs was observed by XRD with CuK$\alpha$ radiation (Perkin-Elmer spectrum). FTIR (Perkin-Elmer 1725X) was used to study the functional group, which is responsible for the reduction of magnesium NPs from plant sample assay. Element composition and morphology of *S. trilobatum* and sodium hydroxide-mediated magnesium NPs

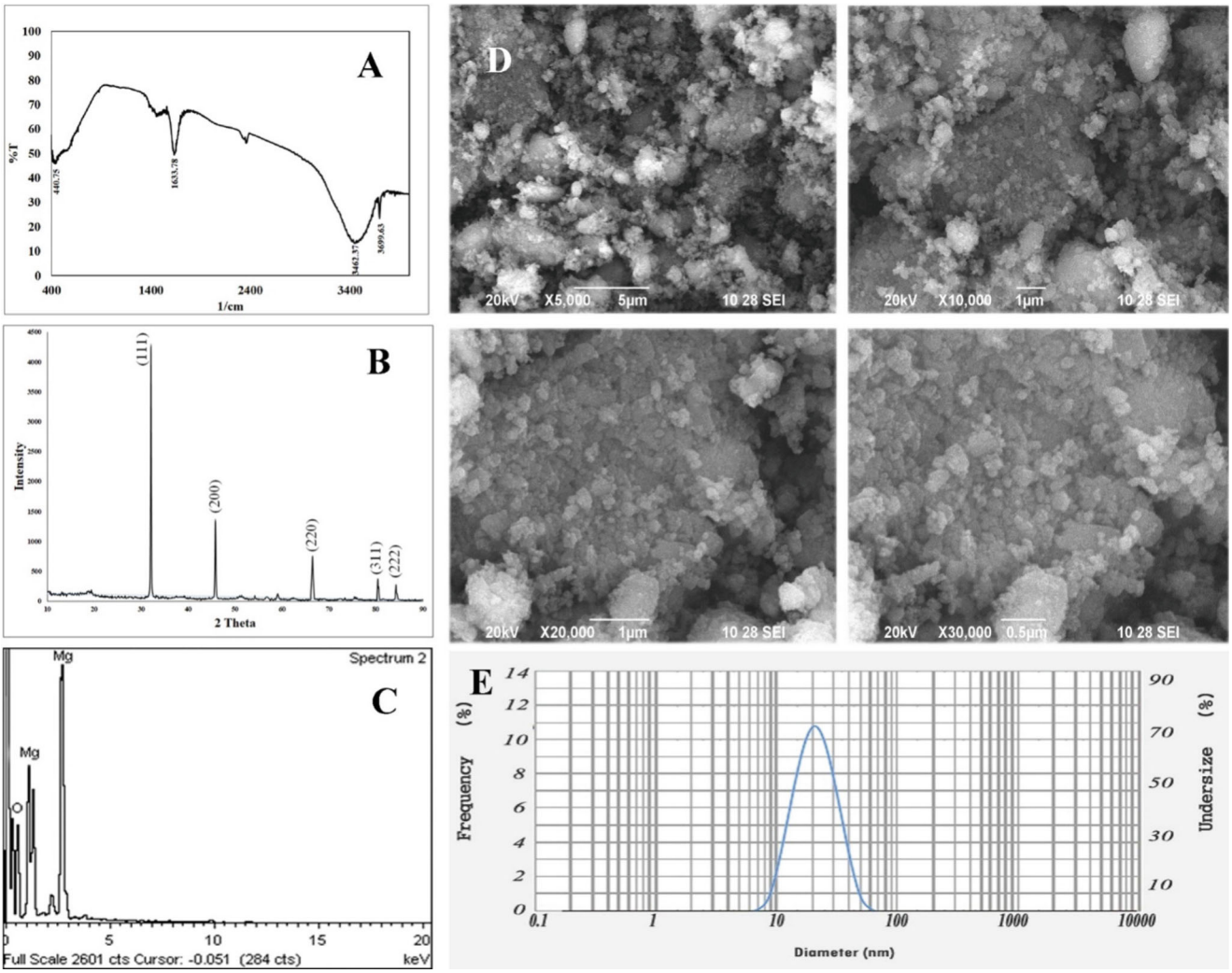


**Figure 3.** Characterization of St-MgO: (**A**) FTIR spectroscopy analysis, (**B**) XRD, (**C**) EDX, (**D**) SEM images of synthesized St-MgO at different resolutions and (**E**) particle-size analysis.

were analysed using EDX (Model QuanTax 200, Germany) and SEM (Model JSM 6390LV), to determine the size of MgO NPs by particle-size analysis [20].

### 3.3 *Antioxidant and antibacterial activities of magnesium NPs*

Antioxidant activity of MgO NPs by DPPH radical scavenging activity was analysed according to the method described by Rai and Ingle *et al* [21], in which DPPH (0.1 mM) reagent taken as a control and the ascorbic acid was used as a standard (lower the absorbance, higher the free radical scavenging activity). Then, the absorbance of the reaction mixture was read at 517 nm with a Shimadzu UV-2450 spectrophotometer. The free radical scavenging activity of the samples was calculated by the formula:

$$\% \text{ Scavenging activity} = \text{Control OD} - \text{Test OD/Control OD} \times 100.$$

Antibacterial activities of *S. trilobatum* and sodium hydroxide-mediated magnesium NPs were determined by the well-diffusion method. Bacterial culture swapped on nutrient agar plate and 5 mm size of well-punched on agar surface with the help of sterile gel puncher. Various concentrations of magnesium NPs such as 25, 50, 75, 100 mg $l^{-1}$ and streptomycin (positive control, 10 $\mu$g $ml^{-1}$) were added in appropriate wells. The plates were incubated at room temperature for 24 h. The zone of inhibition was measured (millimetre in diameter) and mean values were recorded [26,27].

### 3.4 *Statistical analysis*

All results are presented as mean $\pm$ standard deviation (SD). Using SPSS statistical tool, all data were analysed at the significant level $\leq 0.05$ by $t$-test to test the difference between St-MgO, Che-MgO and the control group. One-way analysis of variance (ANOVA) was also performed to test the effect of MgO NPs dose on the test parameters. $P$ values of $\leq 0.05$ were considered statistically significant.

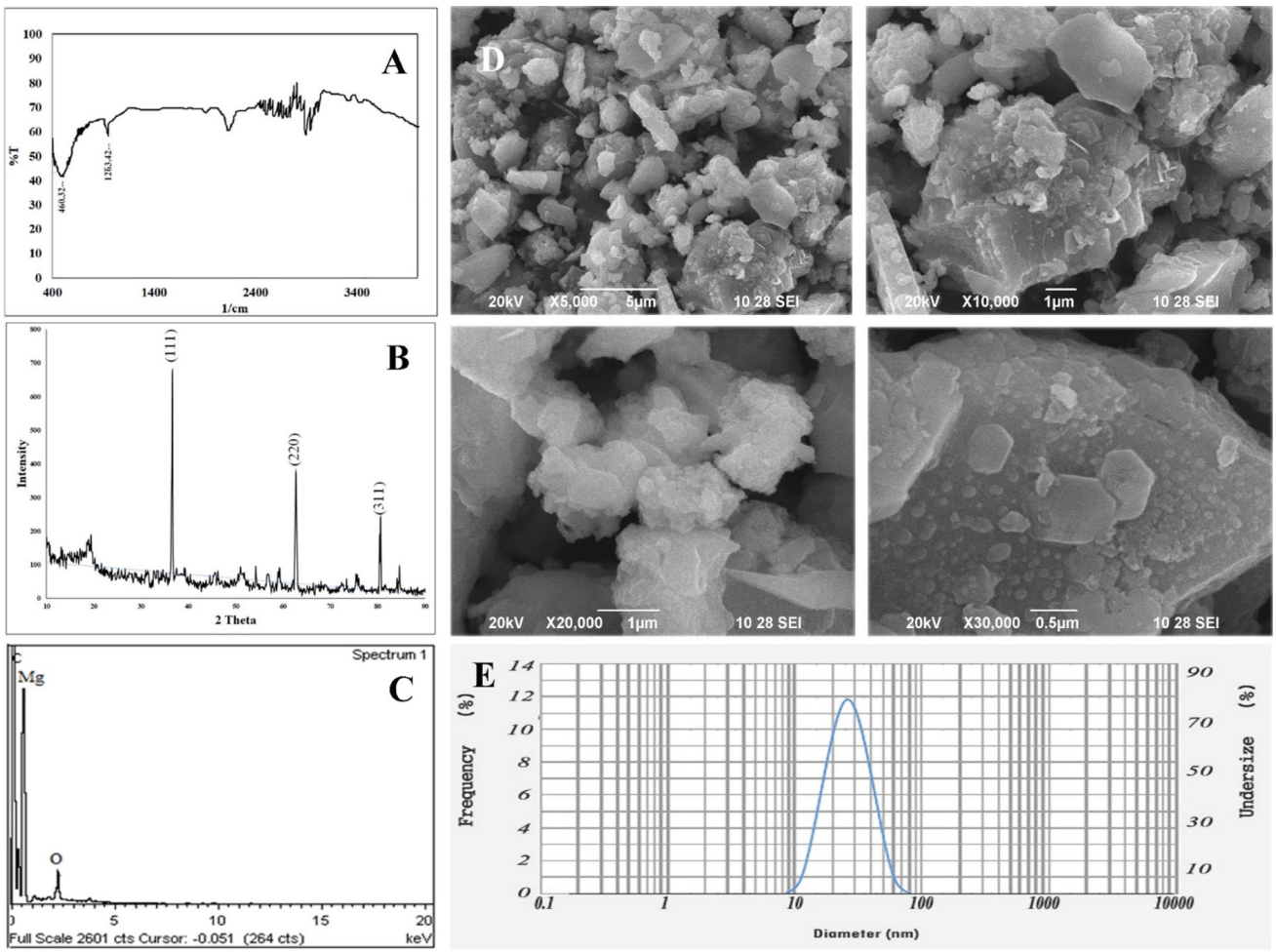


**Figure 4.** Characterization of Che-MgO: (**A**) FTIR spectroscopy analysis, (**B**) XRD, (**C**) EDX (**D**) SEM and (**E**) particle-size analysis.

## 4. Results and discussion

### 4.1 *UV–Vis, FTIR and XRD analyses*

The UV–Vis absorption spectra of St-MgO and Che-MgO are shown in figure 1. UV–Vis absorption spectroscopy is the most widely used method for characterizing the optical properties and electronic structure of NPs, as the absorption bands are related to the diameter and aspect ratio of metal NPs. The absorption spectrum of synthesized St-MgO recorded the peak at 362 nm and colour change observed from brown to pale yellow. For chemical synthesis (Che-MgO), the peak was observed at 374 nm. Palanisamy and Pazhanivel [19] synthesized MgO NPs using betel leaf extract and observed a wide range of optical density at 320 nm. They concluded that synthesis of MgO NPs and band gap of biological synthesis are low when compared to chemical synthesis. Rajeshwari *et al* [22] and Rajiv *et al* [23] described that absorption peak range of 300–400 nm indicates the presence of metal oxide NPs. According to Al-Hazmi *et al* [3], light wavelengths in the range of 300–800 nm are used for characterizing various metal NPs in the size range between 2 and 100 nm. More specifically, the antioxidant properties are related to the number of hydroxyl groups in the particle as well as the level of their esterification. Increase in methyl and hydroxyl group may enhance the antioxidant activity of NPs.

FTIR was used to identify the possible biomolecules which are responsible for the reduction and capping of MgO NPs. FTIR analysis of *S. trilobatum* leaf extract show peaks at 1219.01, 1365.60, 1635.64, 1728.22, 2144.84, 2322.29, 2576.90, 2723.49, 2962.66, 3379.29 and 3950.22 $cm^{-1}$ (figure 2). It corresponds to aliphatic amine (C–N stretch), alkanes (C–H rock), unsaturated ester (C=O stretch), alkynes (–C=C– stretch, C–H stretch), carboxylic acid (O–H stretch), amines (N–H bend), alcohol and phenol (O–H stretch). This functional group acts as reducing and capping agent for the synthesis of MgO NPs.

FTIR analysis determines the functional group which is attached to the surface of St-MgO (figure 3A). The peaks at 440.75, 1633.78, 3462.37 and 3699.63 $cm^{-1}$ refer to N–H bend and O–H stretch. These peaks are responsible for alkyl halide, primary amine, alcohol and phenol group. The strong peaks at 440 and 3699 $cm^{-1}$ was assigned to Mg–O stretching vibration. The remaining peaks (1633 and 3462 $cm^{-1}$) in FTIR spectrum represent stability and capping of MgO NPs. IR spectra of Che-MgO NPs exhibit a high-intensity band around 460.32 and 1263.42 $cm^{-1}$ (figure 4A).

Ganapathi *et al* [7] explained the functional group of magnesium NPs using *Olea europaea* extract in a single step. They concluded that FTIR spectrum peaks at 451 and 3699 $cm^{-1}$ was assigned to MgO NPs. Earlier, Al Hazmi *et al* [3] explained the FTIR spectra of MgO NPs synthesized using *Artemisia abrotanum* herb extract. The spectra showed bands at 3308, 2139, 1635, 1346, 419 and 407 $cm^{-1}$. The strong infrared band near 3308 $cm^{-1}$ was observed for the presence of O–H bond vibrations of the hydroxyl group. The most intense band at 1635 $cm^{-1}$ represents vibrations of C=O, typical for the structure of flavonoids, which can be found in *A. abrotanum* herb extract. The peak which appeared at 2139 $cm^{-1}$ may indicate the presence of alkynes group. The absorption band at 1346 $cm^{-1}$ is related to C–H bonding vibrations of the aromatic tertiary amine group. The peaks observed at 419 and 407 $cm^{-1}$ indicate the presence of MgO NPs. These results suggest that the primary amine function group acts as a capping agent in the formation of MgO NPs.

The XRD techniques are widely used to determine the phase of MgO NPs. Figure 3B shows the XRD profile of St-MgO NPs synthesized using the *S. trilobatum* extract. The XRD strongest peak at $2\theta$ value match with the crystal plane of 39.44° = (111), 45.86° = (200), 66.89° = (220), 80.50° = (311) and 84.89° = (222) of MgO NPs. The $2\theta$ value of NPs found to match with JCPDS-89-4248, confirming the formation of MgO NPs in crystalline nature. For Che-MgO NPs, $2\theta$ value of 36.52° = (111), 62.77° = (220) and 80.60° = (311), which is corresponding to the crystal plane of 111, 220 and 311 found to match with JCPDS-45-0946 (figure 4B). Previously, Ganapathi *et al* [7] described the green synthesis of magnesium NP using orange fruit waste with 21 nm in size. Renata [24] explained the crystal nature of magnesium NPs synthesized from *A. abrotanum* was 10 nm in size and have antioxidant and photocatalytic activities.

### 4.2 *EDX, SEM and particle-size analyses*

The element composition of MgO NPs is analysed using EDX to confirm the purity of NPs. St-MgO NPs have 53.76% of magnesium and 46.23% of oxygen

**Table 1.** Antioxidant activities of St-MgO and Che-MgO nanoparticles.

| Nanoparticles | Concentration ($\mu g\ ml^{-1}$) | Mean ± SD |
|---|---|---|
| St-MgO | 50 | 22.50 ± 0.28 |
| | 100 | 63.83 ± 0.72 |
| | 200 | 81.16 ± 0.60 |
| | 500 | 84.50 ± 0.28 |
| | 1000 | 89.83 ± 0.44 |
| Che-MgO | 50 | 21.00 ± 0.57 |
| | 100 | 59.00 ± 0.57 |
| | 200 | 74.66 ± 1.76 |
| | 500 | 81.16 ± 0.60 |
| | 1000 | 85.50 ± 1.04 |
| Control | 50 | 19.50 ± 0.28 |
| | 100 | 27.16 ± 0.72 |
| | 200 | 42.33 ± 0.88 |
| | 500 | 65.16 ± 0.44 |
| | 1000 | 67.50 ± 1.25 |

Results are expressed in mean ± SD.

**Table 2.** ANOVA test between and within group of control, St-MgO and Che-MgO nanoparticles.

| Nanoparticles | | Sum of square | Mean square | *F* | Sig. |
|---|---|---|---|---|---|
| St-MgO | Between group | 8233.100 | 2058.275 | 656.896 | 0.000* |
| | Within group | 31.333 | 3.133 | | |
| | Total | 8264.433 | | | |
| Che-MgO | Between group | 9027.733 | 2256.933 | 3.009 | 0.000* |
| | Within group | 7.500 | 0.750 | | |
| | Total | 9035.233 | | | |
| Control | Between group | 5658.333 | 1414.583 | 744.518 | 0.000* |
| | Within group | 19.000 | 1.900 | | |
| | Total | 5677.333 | | | |

All the results are statistically significant ($P$ value $\leq 0.05$).
Sig., significant, $^*P \leq 0.05$.

**Table 3.** Antibacterial activity of St-MgO nanoparticles against bacterial pathogens.

| Pathogens | Different concentrations of St-MgO NPs (mg $l^{-1}$) | | | | Control (Streptomycin, 10 $\mu$g $ml^{-1}$) |
|---|---|---|---|---|---|
| | 25 | 50 | 75 | 100 | |
| *E. coli* | 12.00 ± 0.50 | 12.00 ± 1.00 | 13.00 ± 0.50 | 16.66 ± 1.00 | 14.66 ± 1.00 |
| *B. subtilis* | 13.00 ± 1.52 | 13.33 ± 0.59 | 14.00 ± 0.50 | 16.00 ± 1.44 | 13.16 ± 0.50 |
| *S. pyogenes* | 15.16 ± 0.18 | 15.00 ± 0.50 | 15.66 ± 0.45 | 13.66 ± 0.62 | 13.82 ± 0.50 |

The resulted zone of inhibition (mm) is expressed in mean ± SD.

**Table 4.** Antibacterial activity of Che-MgO nanoparticles against bacterial pathogens.

| Pathogens | Different concentrations of Che-MgO NPs (mg $l^{-1}$) | | | | Control (Streptomycin, 10 $\mu$g $ml^{-1}$) |
|---|---|---|---|---|---|
| | 25 | 50 | 75 | 100 | |
| *E. coli* | 12.83 ± 0.76 | 13.00 ± 1.52 | 13.50 ± 0.76 | 15.16 ± 0.63 | 12.83 ± 0.50 |
| *B. subtilis* | 12.50 ± 0.76 | 12.00 ± 1.00 | 14.00 ± 1.04 | 13.00 ± 0.50 | 14.83 ± 0.50 |
| *S. pyogenes* | 13.16 ± 0.83 | 12.33 ± 0.41 | 10.50 ± 0.50 | 13.83 ± 0.78 | 12.62 ± 1.00 |

The resulted zone of inhibition (mm) is expressed in mean ± SD.

(figure 3C). Che-MgO NPs have 83.26% of magnesium and 16.74% of oxygen (figure 4C). The EDX analysis refers to strong signal in the magnesium region of St-MgO and Che-MgO that confirms the presence of MgO NPs.

SEM images of the St-MgO and Che-MgO NPs observed under various magnifications like 5000×, 10,000×, 20,000× and 30,000× (figures 3D and 4D). These figure suggested that St-MgO and Che-MgO NPs are aggregated and are spherical in shape. Particle-size analysis confirmed that the average size of St-MgO and Che-MgO NPs was 30 and 42 nm, respectively (figures 3E and 4E). Krishnamoorthy *et al* [11] synthesized MgO NP exhibited spherical structure with 231 nm size and a small amount of aggregated particles.

### 4.3 *Antioxidant activity of MgO NPs*

The radical scavenging activity of MgO NPs was increased in dose-dependent manner. DPPH scavenging activity of St-MgO NPs is significantly higher with $IC_{50}$ 72.24 $\mu$g $ml^{-1}$ when compared with control ascorbic acid ($IC_{50}$ 33.46 $\mu$g $ml^{-1}$) and Che-MgO NPs ($IC_{50}$ 66.74 $\mu$g $ml^{-1}$) (tables 1 and 2). The leaves of *S. trilobatum* were a rich source of several antioxidant components such as chlorogenic, caffeic, rosmarinic acid, total polyphenols and total flavonoids [15], the NPs synthesized from this source had excellent antioxidant activities. Selvam *et al* [25] demonstrated DPPH scavenging activity by using *Aspergillus flavus*-mediated NPs

**Table 5.** ANOVA for the data on inhibition zone of St-MgO and Che-MgO nanoparticles against bacterial pathogens.

| Pathogens | Nanoparticles | | Sum of square | Mean square | *F* | Sig. |
|---|---|---|---|---|---|---|
| *E. coli* | St-MgO | Between group | 32.250 | 10.750 | 17.200 | 0.001* |
| | | Within group | 5.00 | 0.625 | | |
| | | Total | 37.250 | | | |
| | Che-MgO | Between group | 15.945 | 5.315 | 5.455 | 0.003* |
| | | Within group | 7.794 | 0.947 | | |
| | | Total | 23.739 | | | |
| *B. subtilis* | St-MgO | Between group | 15.092 | 5.031 | 5.106 | 0.029* |
| | | Within group | 7.881 | 2.333 | | |
| | | Total | 22.973 | | | |
| | Che-MgO | Between group | 7.833 | 2.611 | 3.581 | 0.066 |
| | | Within group | 5.833 | 3.708 | | |
| | | Total | 13.667 | | | |
| *S. pyogenes* | St-MgO | Between group | 7.642 | 2.547 | 11.489 | 0.003* |
| | | Within group | 1.774 | 2.316 | | |
| | | Total | 9.416 | | | |
| | Che-MgO | Between group | 29.459 | 9.820 | 4.427 | 0.041* |
| | | Within group | 17.746 | 2.218 | | |
| | | Total | 47.205 | | | |
| Control | | Between group | 22.220 | 4.444 | 2.774 | 0.039* |
| | | Within group | 19.223 | 4.913 | | |
| | | Total | 41.444 | | | |

All the results are statistically significant except Che-MgO NPs against *Bacillus* ($P$ value $\leq 0.05$).
Sig., significant, $*P < 0.05$.

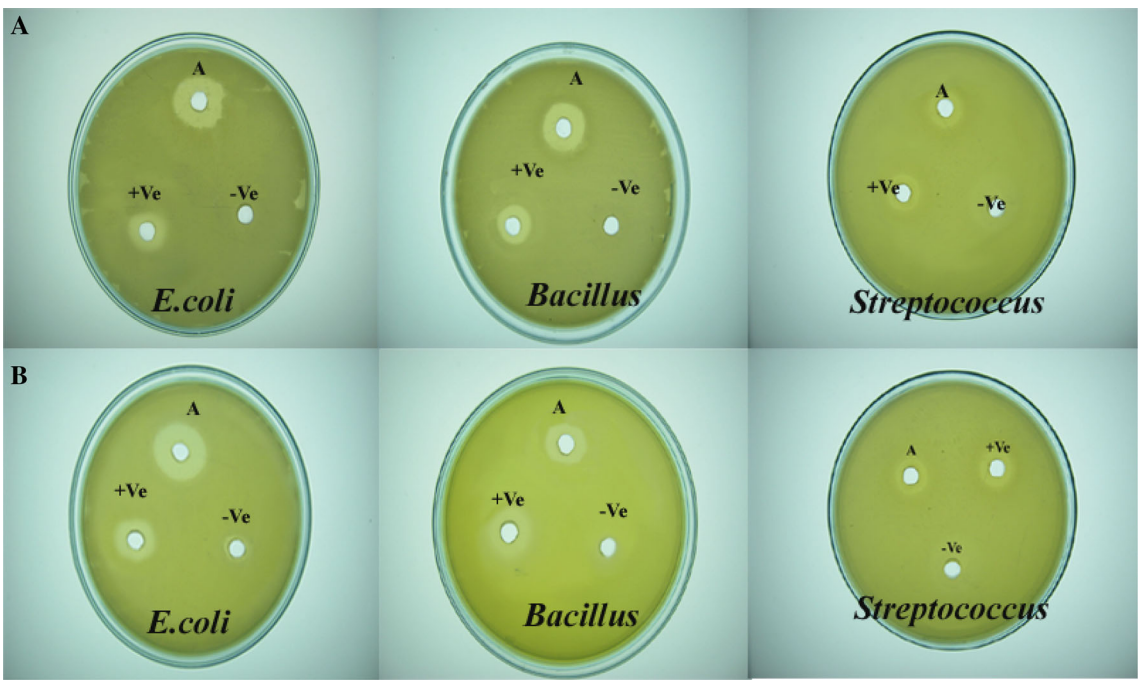


**Figure 5.** Antibacterial activity of (**A**) St-MgO and (**B**) Che-MgO nanoparticles against *E. coli*, *B. subtilis* and *S. pyogenes*. A, 100 mg $ml^{-1}$ concentration of MgO NPs, +Ve, 10 $\mu g\ ml^{-1}$ concentration of streptomycin (positive control), -Ve, Millipore water (negative control).

showing 80% activity at 400 $\mu g\ ml^{-1}$. In another study, silver NPs synthesized from the leaf extract of *Excoecaria agallocha* showed 90% DPPH scavenging activity at 1 $mg\ ml^{-1}$ concentration [2].

### 4.4 *Antibacterial activity of MgO NPs*

*S. trilobatum* and sodium hydroxide-mediated MgO NPs show an excellent antibacterial activity against bacterial pathogens. The highest zone of inhibition was observed in St-MgO against *E. coli* with a diameter of $16.66 \pm 0.66$ mm at a concentration of 100 $mg\ ml^{-1}$ and the lowest inhibition was observed in *S. pyogenes* with a zone diameter of $13.66 \pm 2.08$ mm at the same concentration (table 3). *S. trilobatum*-mediated MgO NPs showed effective antibacterial activity in *E. coli*. Likewise, Che-MgO NPs show maximum zone of inhibition observed in *E. coli* ($15.16 \pm 0.44$ mm) and a minimum zone of inhibition in *S. pyogenes* ($13.83 \pm 0.92$ mm) at a concentration of 100 $mg\ ml^{-1}$ (tables 4 and 5). Figure 5 shows the antibacterial activity of St-MgO and Che-MgO NPs against bacterial pathogens at a concentration of 100 $mg\ ml^{-1}$. Doss *et al* [6] explained that the antibacterial activity of MgO NPs against *E. coli* was due to a broad range of oxygen present on the surface of magnesium. Krishnamoorthy *et al* [11] described the effect of magnesium NPs against Gram-positive and Gram-negative bacteria with the minimum inhibitory concentration of 500 $\mu g\ ml^{-1}$ against *Pseudomonas* and *E. coli*. Doss *et al* [6] and Krishnamoorthy *et al* [11] explained the enhanced antibacterial activity of magnesium NPs due to ROS and lipid peroxide with a defect of oxygen present on the morphology of particles. MgO NPs, strong in electrostatic interaction with bacterial surface led to cell death [28,29].

## 5. Conclusion

The present study reported that MgO NPs synthesized by precipitation method using sodium hydroxide and *S. trilobatum* leaf extract act as a capping and reducing agent with magnesium nitrate precursor. Synthesized *S. trilobatum*-mediated MgO NPs are spherical in shape and is $30 \pm 6$ nm in size. MgO NPs capped with *S. trilobatum* have excellent antioxidant properties. Also, it shows promising antibacterial activity against *E. coli* and *B. subtilis* at a concentration of 100 $\mu g\ ml^{-1}$. Thus, we conclude *S. trilobatum*-mediated MgO NPs can be used to treat the diseases caused by free radicals.

## Acknowledgements

We acknowledge the management of Sri Krishna Arts and Science College, Coimbatore, Tamil Nadu, India, for providing necessary facilities to carry out this study.

## References

[1] Alaa Y G, Tawfiq M A, Akl M M and Muhand W A 2017 *ARPN J. Agric. Biol. Sci.* **10** 293
[2] Al-Gaashani R, Radiman S, Al-Douri Y, Tabet N and Daud A R 2012 *J. Alloys Compd.* **52** 71
[3] Al-Hazmi F, Alnowaiser F, Al-Ghamdi A A, Aly M M, Al-Tuwirqi R M and El-Tantawy F 2012 *Superlattices Microstruct.* **52** 200
[4] Alvarado E, Torres-Martinez L M and Fuentes A F 2000 *Polyhedron* **19** 2345
[5] Bhatte K D, Sawant D N, Watile R A and Bhanage B M 2012 *Mater. Lett.* **69** 66
[6] Doss A, Muhamed M H and Dhanabalan R 2009 *Indian J. Sci. Tech.* **2** 41
[7] Ganapathi R K, Ashok C H, Venkateswara R K, Shilpa Chakra C H and Akshaykranth A 2015 *Int. J. Adv. Res. Phys. Sci.* **2** 1
[8] Huang L, Li D Q, Lin Y J, Evans D G and Duan X 2005 *Chin. Sci. Bull.* **50** 514
[9] Jawhar M, Amalan R G and Jeyaseelan M 2004 *Plant Tissue Cult. Biotechnol.* **14** 107
[10] Kanchana D, Jayanthi M, Kanchana D, Saranraj P and Sujitha D 2013 *Int. J. Microbiol. Res.* **4** 300
[11] Krishnamoorthy K, Manivannan G, Kim S J, Jeyasubramanian K and Premanathan M 2012 *J. Nanoparticle Res.* **14** 1063
[12] Kumar D, Reddy Yadav L S, Lingaraju K, Manjunath K, Suresh D, Prasad D *et al* 2015 *AIP Conf. Proc.* **1665** 050145
[13] Li Y J, Li D Q, Wang G, Huang L and Duan X 2005 *J. Mater. Sci. Mater. Med.* **16** 53
[14] Vanaja M, Paulkumar K, Baburaja M, Rajeshkumar S, Gnanajobitha G, Malarkodi C *et al* 2014 *Bioinorg. Chem. Appl.* **2014** 8
[15] Marina Z, Mariana P, Thiele F B, Aline A B, Robson B F, Michel M M *et al* 2012 *Molecules* **17** 12560
[16] Narendhran S, Rajiv P, Vanathi P and Rajeshwari S 2014 *Int. J. Pharm. Pharm. Sci.* **6** 319
[17] Narendhran S, Rajiv P and Rajeshwari S 2016 *Bull. Mater. Sci.* **39** 1
[18] Pacholski C, Kornowski A and Weller H 2002 *Angew. Chem. Int. Ed.* **41** 1188
[19] Palanisamy G and Pazhanivel T 2017 *Int. Res. J. Eng. Tech.* **4** 137
[20] Raghupati R K, Koodali R T and Manna A C 2011 *Langmuir* **27** 4020
[21] Rai M and Ingle A 2012 *Appl. Microbiol. Biotechnol.* **94** 287
[22] Rajeshwari S, Rahman P K S M, Rajiv P, Narendhran S and Venckatesh R 2014 *Spectrochim. Acta Part A* **129** 255
[23] Rajiv P, Rajeshwari S and Venckatesh R 2013 *Spectrochim. Acta Part A* **112** 384
[24] Renata D 2016 *Iran. J. Sci. Technol. A* **1** 9
[25] Selvam N C S, Kumar R T, Kennedy L J and Vijaya J J 2011 *J. Alloys Compd.* **509** 9809
[26] Shahjahan M, Sabitha K E, Jamu M and Shyamala Devi C S 2004 *Indian J. Med. Res.* **120** 194
[27] Sri Vishnupriya R, Narendhran S and Rajeshwari S 2016 *Bull. Mater. Sci.* **39** 361
[28] Stoimenov P K, Klinger R L, Marchin G L and Klabunde K J 2002 *Langmuir* **18** 6679
[29] Sundrarajan M, Suresh J and Gandhi R R 2012 *Dig. J. Nanomater. Biostruct.* **7** 983